The EMBO Journal (2011) 30, 2934–2947 | © 2011 European Molecular Biology Organization | All Rights Reserved 0261-4189/11
www.embojournal.org

THE EMBO JOURNAL

Identity, regulation and *in vivo* function of gut NKp46$^+$RORγt$^+$ and NKp46$^+$RORγt$^-$ lymphoid cells

Ana Reynders[1,2,3], Nadia Yessaad[1,2,3], Thien-Phong Vu Manh[1,2,3], Marc Dalod[1,2,3], Aurore Fenis[1,2,3], Camille Aubry[4,5,6], Georgios Nikitas[5,7], Bertrand Escalière[1,2,3], Jean Christophe Renauld[8], Olivier Dussurget[4,5,6], Pascale Cossart[4,5,6], Marc Lecuit[5,7,9], Eric Vivier[1,2,3,10,*] and Elena Tomasello[1,2,3,*]

[1]Centre d'Immunologie de Marseille-Luminy, Université de la Mediterannée, Campus du Luminy, Marseille, France, [2]Institut National de la Santé et de la Recherche Medicale U631, Marseille, France, [3]Centre National de la Recherche Scientifique, Unite Mixte de Recherche 6102, Marseille, France, [4]Unité des Interactions Bactéries-Cellules, Department of Cellular Biology and Infection, Institut Pasteur, Paris, France, [5]Inserm U604, Paris, France, [6]INRA USC2020, Paris, France, [7]Microbes and Host Barriers Group, Department of Infection and Epidemiology, Institut Pasteur, Paris, France, [8]Ludwig Institute for Cancer Research Ltd, Experimental Medicine Unit, Universite Catholique de Louvain, Brussels, Belgium, [9]Université Paris Descartes, Centre d'Infectiologie Necker-Pasteur, Service des Maladies Infectieuses et Tropicales, Hôpital Necker-Enfants Malades, Assistance Publique-Hôpitaux de Paris, Paris, France and [10]Assistance Publique des Hôpitaux de Marseille, Hôpital de la Conception, Marseille, France

The gut is a major barrier against microbes and encloses various innate lymphoid cells (ILCs), including two subsets expressing the natural cytotoxicity receptor NKp46. A subset of NKp46$^+$ cells expresses retinoic acid receptor-related orphan receptor γt (RORγt) and produces IL-22, like lymphoid tissue inducer (LTi) cells. Other NKp46$^+$ cells lack RORγt and produce IFN-γ, like conventional Natural Killer (cNK) cells. The identity, the regulation and the *in vivo* functions of gut NKp46$^+$ ILCs largely remain to be unravelled. Using pan-genomic profiling, we showed here that small intestine (SI) NKp46$^+$RORγt$^-$ ILCs correspond to SI NK cells. Conversely, we identified a transcriptional programme conserved in fetal LTi cells and adult SI NKp46$^+$RORγt$^+$ and NKp46$^-$RORγt$^+$ ILCs. We also demonstrated that the IL-1β/IL-1R1/MyD88 pathway, but not the commensal flora, drove IL-22 production by NKp46$^+$RORγt$^+$ ILCs. Finally, oral *Listeria monocytogenes* infection induced IFN-γ production in SI NK and IL-22 production in NKp46$^+$RORγt$^+$ ILCs, but only IFN-γ contributed to control bacteria dissemination. NKp46$^+$ ILC heterogeneity is thus associated with subset-specific transcriptional programmes and effector functions that govern their implication in gut innate immunity.

*Corresponding authors. E Vivier or E Tomasello, Centre d'Immunologie de Marseille-Luminy, CIML, Université de la Mediterannée, Campus du Luminy, Case 906, Marseille 13288, France. Tel.: +33 49 126 9412; Fax: +33 49 126 9430; E-mail: vivier@ciml.univ-mrs.fr or Tel.: +33 49 126 9432; Fax: +33 49 126 9430; E-mail: tomasell@ciml.univ-mrs.fr

Received: 24 January 2011; accepted: 26 May 2011; published online: 17 June 2011

The EMBO Journal (2011) **30,** 2934–2947. doi:10.1038/emboj.2011.201; Published online 17 June 2011
Subject Categories: immunology
Keywords: gut immunosurveillance; innate lymphoid cells; *Listeria monocytogenes*; NKp46; RORγt

Introduction

Epithelial tissues represent a physical barrier to various assaults and regulate immune responses (Swamy *et al*, 2010). In the intestine, signals emanating from epithelial cells and luminal contents constantly regulate gut-associated lymphoid tissue (GALT) development and function, thereby contributing to maintain a 'tolerogenic' status to innocuous antigens and commensal flora while initiating immune responses that restrain pathogen invasion (Iwasaki, 2007; Abreu, 2010). In parallel, the immune system has developed several strategies to preserve and restore epithelial barrier integrity, in part through IL-22 production (Wolk *et al*, 2010). The complexity of gut cells that participate to mucosal immunity has recently emerged via the identification of several subsets of innate lymphoid cells (ILCs) (Spits and Di Santo, 2011).

ILCs include IL-25-R$^+$ and IL-33-R$^+$ cells, such as natural helper cells (Moro *et al*, 2010), nuocytes (Neill *et al*, 2010) and multipotent progenitors (Saenz *et al*, 2010), which secrete IL-4, IL-5 and IL-13 type-2 cytokines and are involved in the control of worm gastrointestinal infection. Other subsets of ILCs express the retinoic acid receptor-related orphan receptor γt (RORγt) transcription factor. RORγt has been first shown to characterize lymphoid tissue inducer (LTi) cells that orchestrate lymphoid organogenesis (Mebius, 2003; Ivanov *et al*, 2006) and represent a major innate source of IL-22 in both mice (Ivanov *et al*, 2008) and humans (Cupedo *et al*, 2009). Besides, Sca-1$^+$RORγt$^+$ ILCs drive intestinal immunity and immunopathology by secreting the pro-inflammatory cytokines IL-17 and IFN-γ (Buonocore *et al*, 2010). Like LTi cells, other RORγt$^+$ cells expressing natural killer (NK) markers, such as NKp46, produce IL-22. Mouse NKp46$^+$RORγt$^+$ cells are localized in the gut (Satoh-Takayama *et al*, 2008; Cella *et al*, 2009; Luci *et al*, 2009; Sanos *et al*, 2009), while their human counterparts have been detected in gut and tonsils (Cella *et al*, 2009; Cupedo *et al*, 2009; Hughes *et al*, 2009; Crellin *et al*, 2010; Takayama *et al*, 2010). Finally, gut NKp46$^+$RORγt$^-$ cells able to produce IFN-γ, like conventional NK (cNK) cells, have also been described in the gut (Satoh-Takayama *et al*, 2008; Cella *et al*, 2009; Luci *et al*, 2009; Sanos *et al*, 2009).

Several issues regarding IL-22-secreting gut NKp46$^+$RORγt$^+$ and NKp46$^-$RORγt$^+$ cells as well as IFN-γ-producing NKp46$^+$RORγt$^-$ gut ILCs remain to be unveiled. In particular, while it is known that IL-22 produced by RORγt$^+$ cells is crucial for mice survival upon colonic *Citrobacter rodentium* infection (Satoh-

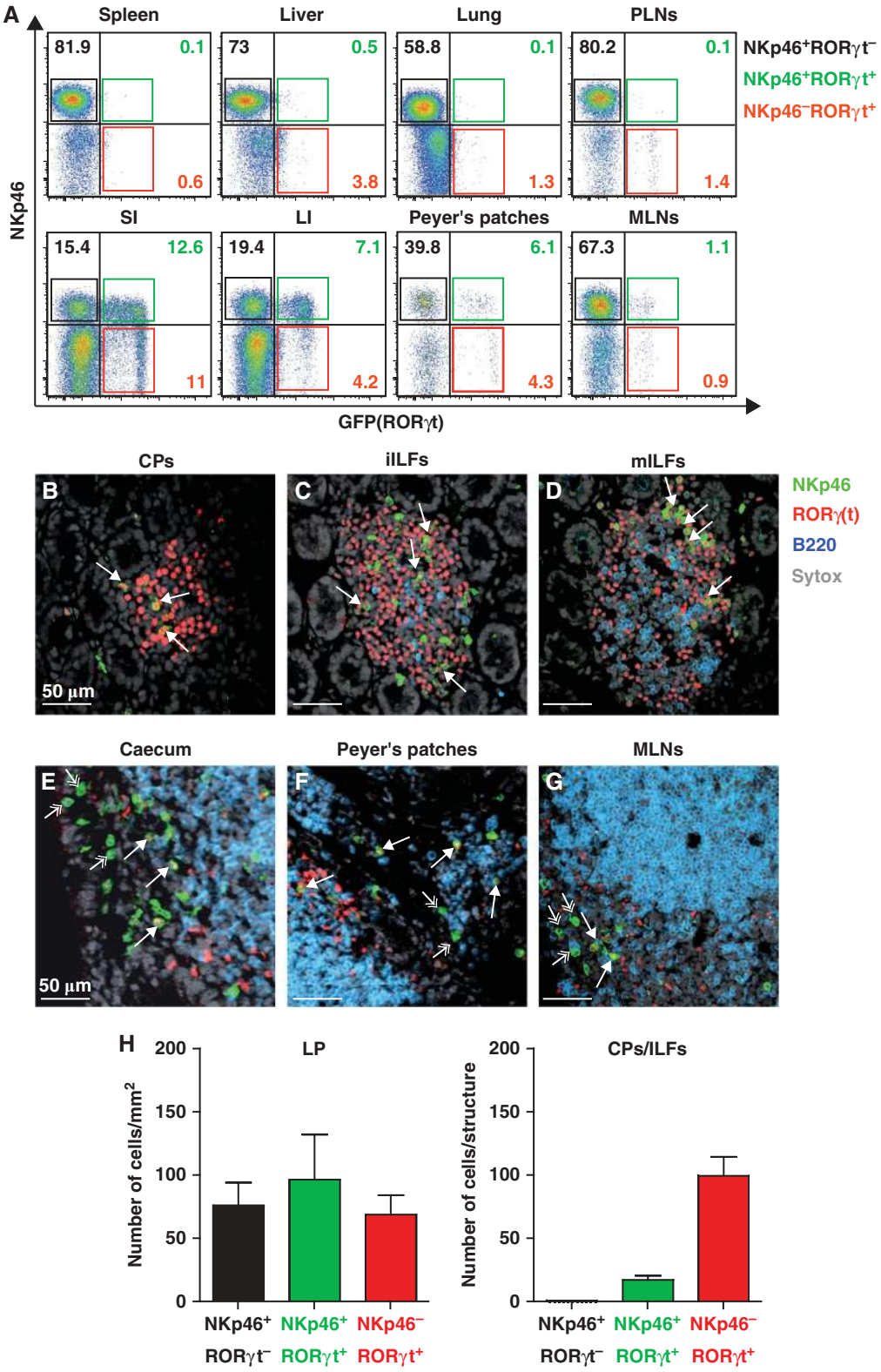

Figure 1 Tissue distribution of NKp46$^+$RORγt$^-$ and NKp46$^+$RORγt$^+$ cells. (**A**) Flow cytometry analysis of cells isolated from the indicated organs of RORc(γt)$^{+/GFP}$ reporter mice, by gating on CD45$^+$CD3$^-$CD19$^-$ cells. Numbers in quadrants indicate percentage of cells. Black boxes: NKp46$^+$RORγt$^-$; green boxes: NKp46$^+$RORγt$^+$; red boxes: NKp46$^-$RORγt$^+$. SI, small intestine; LI, large intestine; MLN, mesenteric LN; PLN, peripheral LN. One experiment representative of three is depicted. (**B–G**) Frozen sections of small and large intestine, PPs and MLNs stained with polyclonal anti-NKp46 serum (green), anti-RORγ supernatant hybridoma (red) and anti-B220 (blue). Nuclei were counterstained with Sytox (grey). Filled arrows indicate NKp46$^+$RORγt$^+$ cells, while double-tip arrows indicate NKp46$^+$RORγt$^-$ cells. Scale bar = 50 μm. Data are representative of at least three independent experiments. (**H**) NKp46$^+$RORγt$^-$, NKp46$^+$RORγt$^+$ and NKp46$^-$RORγt$^+$ cells detectable in LP, CPs and ILFs were quantified in SI sections isolated from three (left) or from five (right) B6 mice. Counting of the indicated cell subsets was performed in 35 distinct areas of the SI LP (left) or in 26 distinct lymphoid structures (right) of tissue sections. Cell numbers/mm^2 within LP or cell numbers/structure (CPs/ILFs) are expressed as mean ± s.e.m.

Takayama *et al*, 2008; Cella *et al*, 2009), the contributions of NKp46$^+$RORγt$^+$ and NKp46$^-$RORγt$^+$ cells are unknown. Furthermore, the distribution of NKp46$^+$RORγt$^+$ and NKp46$^+$RORγt$^-$ within the GALT, as well as the role of commensal flora in their development, remain a matter of debate (Satoh-Takayama *et al*, 2008; Luci *et al*, 2009; Sanos *et al*, 2009; Sawa *et al*, 2010; Vonarbourg *et al*, 2010). Moreover, the lineage relationship of NKp46$^+$RORγt$^+$ and NKp46$^+$RORγt$^-$ cells with LTi cells and cNK cells, respectively, is still unclear (Luci *et al*, 2009; Sanos *et al*, 2009; Vivier *et al*, 2009; Satoh-Takayama *et al*, 2010). In this study, we investigated these issues by comparing the anatomical, transcriptional and functional features of small intestine (SI) NKp46$^+$RORγt$^-$ and NKp46$^+$RORγt$^+$ cells at steady state and upon oral *Listeria monocytogenes* (*L.m.*) infection, a model microorganism that is able to actively cross the intestinal epithelial barrier, to reach the lamina propria (LP) and to disseminate to the systemic circulation.

Results

Tissue distribution of NKp46$^+$RORγt$^-$ and NKp46$^+$RORγt$^+$ cells

IL-22-secreting ILCs have been recently reported in spleen, lymph nodes (LNs) and lungs (Zenewicz *et al*, 2008; Takatori *et al*, 2009; Guo and Topham, 2010). As NKp46$^+$RORγt$^+$ cells secrete IL-22, we analysed the distribution of NKp46$^+$RORγt$^+$ ILCs in lymphoid and non-lymphoid tissues isolated from RORc(γt)$^{+/GFP}$ reporter mice (Eberl *et al*, 2004), in comparison to NKp46$^-$RORγt$^+$ and NKp46$^+$RORγt$^-$ cells. Using flow cytometry, NKp46$^+$RORγt$^-$ cells were found broadly distributed in all tissues studied (Figure 1A). In contrast, NKp46$^+$RORγt$^+$ and NKp46$^-$RORγt$^+$ ILCs were mostly found in the LP of both small and large intestine, in Peyer's patches (PPs) and mesenteric LNs (MLNs), but barely detectable outside of the gut, with the exception of rare NKp46$^-$RORγt$^+$ cells in peripheral LNs (Figure 1A).

We then investigated by immunofluorescence the precise localization of NKp46$^-$RORγt$^+$, NKp46$^+$RORγt$^+$ and NKp46$^+$RORγt$^-$ cells within the GALT. While several studies agree on the localization of both NKp46$^+$RORγt$^-$ and NKp46$^+$RORγt$^+$ cells in LP, the presence of NKp46$^+$RORγt$^+$ cells in cryptopatches (CPs) and CP-derived isolated lymphoid follicles (ILFs) is debated (Satoh-Takayama *et al*, 2008; Luci *et al*, 2009; Sanos *et al*, 2009). To address this issue, we established the validity of the use of the polyclonal anti-mouse NKp46 serum by flow cytometry and tissue immunofluorescence. Indeed, the staining obtained with this reagent was restricted to CD3$^-$NK1.1$^+$ cells in flow cytometry (Supplementary Figure S1A) and was abrogated in tissue immunofluorescence by mouse NKp46-Fc chimeric recombinant protein (Supplementary Figure S1B). Using this protocol, NKp46$^+$RORγt$^+$ cells and NKp46$^-$RORγt$^+$ cells were detected in CPs and ILFs at different degrees of maturation (Figure 1B–D). NKp46$^+$RORγt$^+$ cells were scattered within CPs and immature ILFs (iILFs) (Figure 1B and C), but were localized in the periphery of B-cell areas in mature ILFs (mILFs) (Figure 1D), thus suggesting that the location of these cells changes according to the degree of maturation of these lymphoid structures. NKp46$^+$RORγt$^+$ cells and NKp46$^-$RORγt$^+$ cells were also found in caecal lymphoid structures (Figure 1E), as well as in the interfollicular region of PPs and in the paracortical region of MLNs, in particular beneath and between B-cell follicles (Figure 1F and G). We quantified NKp46$^+$RORγt$^-$, NKp46$^+$RORγt$^+$ and NKp46$^-$RORγt$^+$ cells in LP as well as in CPs and ILFs (Figure 1H). The three populations were equally distributed within LP, while NKp46$^-$RORγt$^+$ ILCs were predominant in CPs/ILFs. Within these structures, the majority of NKp46$^-$RORγt$^+$ cells were CD3$^-$, while in LP we detected both CD3$^-$ and CD3$^+$ RORγt$^+$ ILCs (Supplementary Figure S1C). NKp46$^+$RORγt$^+$ cells were present in both localizations, but they were quantitatively more abundant in LP (Figure 1H).

Thus, at steady state, NKp46$^+$RORγt$^+$ cells were mainly restricted to the GALT and often colocalized with NKp46$^-$RORγt$^+$ cells within organized lymphoid structures. In contrast, NKp46$^+$RORγt$^-$ cells were extremely rare within GALT lymphoid aggregates, although they could be found in the parafollicular region of caecal lymphoid patches, PPs and MLNs (Figure 1E–G).

Genome-wide expression profiling of SI NKp46$^+$RORγt$^-$ and NKp46$^+$RORγt$^+$ cells

NKp46$^+$RORγt$^-$ and NKp46$^+$RORγt$^+$ cells share with cNK cells and LTi cells, respectively, cell surface markers, effector functions and developmental pathways (Luci *et al*, 2009; Sanos *et al*, 2009; Satoh-Takayama *et al*, 2010). We therefore used genome-wide expression profiling to assess the global similarity among these different cell populations. NKp46$^+$RORγt$^-$ (NKp46$^+$GFP$^-$) cells, NKp46$^+$RORγt$^+$ cells (NKp46$^+$GFP^{low} and NKp46$^+$GFP^{high} cells) and NKp46$^-$RORγt$^+$ (NKp46$^-$GFP$^+$) ILCs, which include adult LTi cells (Sawa *et al*, 2010), were sorted by flow cytometry from CD3$^-$ LP cells of SI of RORc(γt)$^{+/GFP}$ reporter mice (Figure 2A). Splenic NKp46$^+$RORγt$^-$ (NKp46$^+$GFP$^-$) cells were also sorted as the reference for cNK cells (Figure 2A). For each cell subset, two independent samples were generated and

Figure 2 Hierarchical clustering of SI NKp46$^+$ cell subsets. (**A**) SI LPCs or splenocytes isolated from Rorc(γt)$^{+/GFP}$ mice were sorted as depicted by gating on CD45$^+$CD3$^-$CD19$^-$ cells. Numbers within boxes indicate corresponding cell subsets: 1 = SI NKp46$^+$RORγt$^-$; 2 = SI NKp46$^+$RORγt^{low}; 3 = SI NKp46$^+$RORγt^{high}; 4 = SI NKp46$^-$RORγt$^+$; 5 = spleen NKp46$^+$RORγt$^-$. Data are representative of two independent experiments. (**B**) Hierarchical clustering with average linkage was performed on normalized microarray data obtained from duplicates of each cell subset indicated. Dendrogram was obtained by using selected 26 963 probesets, as explained in Supplementary data. Numbers at the right side of the dendrogram indicate the cell subsets, as in (**A**), followed by number of duplicate (0.1 or 0.2). Boxes enclose clusters regrouping RORγt$^-$ (green) or RORγt$^+$ (red) cell subsets. (**C**) Heatmap representation of the genes with the most robust differential expression patterns across cell types. 2209 probesets were selected based on their high and consistent differential expression between cell subsets as assessed by *K*-means analyses and explained in Supplementary data. Unsupervised hierarchical clustering with average linkage confirmed the existence of eight major distinct gene expression patterns across the five cell subsets examined, as indicated by Roman letters on the right side of the heatmap. Yellow denotes median expression level across all cell types; red denotes high expression, above median; and blue denotes low expression, below median. (**D**, **E**) Functional categories obtained upon David software analysis of genes included in cluster I (**D**) or cluster V (**E**) were ranked from the most (top) to the least (bottom) statistically representative (*P*-value <0.05). Numbers (Nb.) of genes included in each category are shown. Microarray datasets have been deposited in the Gene Expression Omnibus (GEO) database under reference number GSE29777.

found to cosegregate in hierarchical clustering (Figure 2B). This result validated the quality of our data for assessing the relationships between cell subsets based on their overall transcriptional similarity. The hierarchical clustering analysis generated two distinct cell clusters, the first regrouping SI NKp46$^+$RORγt$^-$ cells with splenic NK cells and the second SI NKp46$^+$RORγt$^+$ cells with NKp46$^-$RORγt$^+$ ILCs (Figure 2B). These results thus showed that the combined expression of RORγt and NKp46 is a major discriminating factor to identify distinct SI ILC subsets, with NKp46$^+$RORγt$^-$ cells resembling cNK cells, and NKp46$^+$RORγt$^+$ cells resembling NKp46$^-$RORγt$^+$ cells.

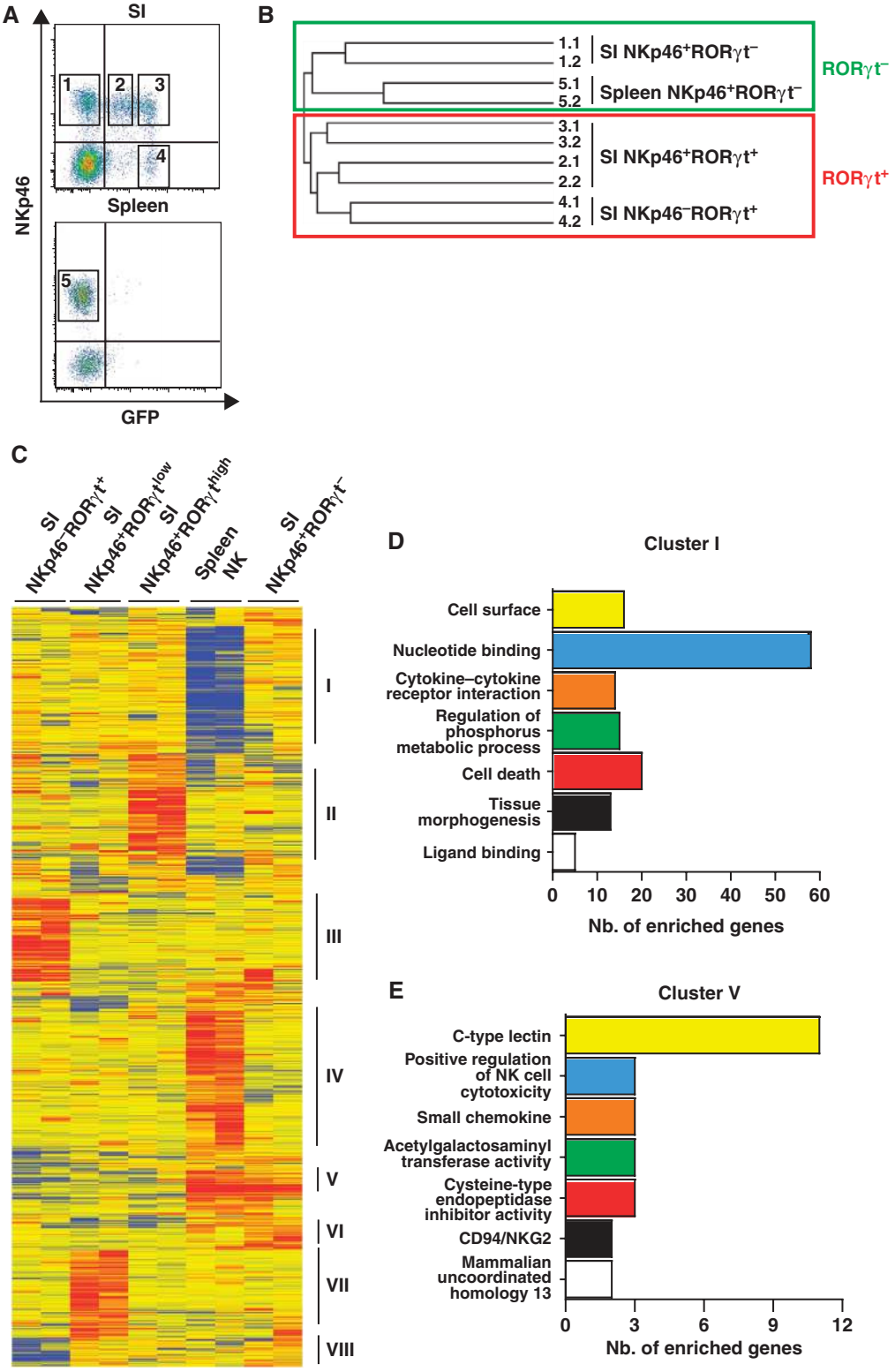

To gain further insights into the relationships between cNK cells, NKp46$^+$RORγt$^-$, NKp46$^+$RORγt$^+$ and NKp46$^-$RORγt$^+$ cells, we selected, clustered and annotated the genes harbouring the most robust and consistent differential expression patterns across cell types (see Supplementary data). A hierarchical clustering based on selected genes revealed eight major clusters of genes (Figure 2C; Supplementary Table SI). The highest numbers of functional annotations were obtained upon analysis of genes included in clusters I and V (Figure 2D and E; Supplementary Tables SII and SIII; for functional annotation analysis and gene lists of the other clusters see Supplementary data, Supplementary Figure S2 and Supplementary Tables SIV–SIX). Cluster I corresponded to genes expressed to lower levels in splenic NK cells ($n=274$; Figure 2C; Supplementary Table SII). The most statistically enriched annotations for cluster I (Figure 2D) included 'nucleotide binding', 'cytokine/cytokine receptor interaction' and 'ligand binding'. While the roles of the genes in the first category in SI ILC biology remain to be explored, the two other annotation groups encompassed most of the genes known to be involved in LTi cell development and function (e.g. *Il22*, *Il2ra*, *Il4ra*, *Il23r*, *Il7r*, *kit*, *Tnfsf11*, and *Rorc* and *Rora*, respectively; Supplementary Figure S2E). Cluster V corresponded to genes expressed at higher levels in both SI NKp46$^+$RORγt$^-$ and spleen NK cells ($n=78$; Figure 2C; Supplementary Table SIII). Functional annotations statistically enriched in cluster V included 'C-type lectins' and 'positive regulation of NK cell cytotoxicity' corresponding largely to genes encoding Ly49 and other KLR molecules, typically expressed by cNK cells. Hence, as compared with the other SI cell types studied, SI NKp46$^+$RORγt$^-$ cells selectively overexpressed many genes characteristic of cNK cells (Figure 2E; Supplementary Figure S2F).

We sought to challenge our findings that SI NKp46$^+$RORγt$^-$ cells resembled cNK cells, and to further advance our characterization of NKp46$^+$RORγt$^+$ cells with respect to *bona fide* fetal LTi cells. Towards this aim, we defined NK cell-specific and fetal LTi cell-specific gene sets by mining published microarray data for 14 different haematopoietic cell types (see Supplementary data and Supplementary Tables SX and SXI). We then re-analysed our microarray data by performing Gene Set Enrichment Analyses (GSEA) to assess whether NK or fetal LTi gene signatures were statistically enriched in pairwise comparisons between the SI ILC subsets. We first validated our approach by showing that splenic NK cells preferentially expressed the NK gene set, when compared with all the SI ILC subsets studied (Figure 3A; Supplementary Figure S3A; Supplementary Table SX), while the fetal LTi gene set was significantly enriched in all SI RORγt$^+$ ILCs, but not in NKp46$^+$RORγt$^-$ cells (Figure 3B; Supplementary Figure S3B; Supplementary Table SXI). In pairwise comparison between SI NKp46$^+$ ILCs and SI NKp46$^-$RORγt$^+$ cells, all SI NKp46$^+$ ILCs preferentially expressed the NK gene set (Figure 3A; Supplementary Figure S3C and E; Supplementary Table SX). Fetal LTi genes were significantly enriched when comparing SI NKp46$^-$RORγt$^+$ to SI NKp46$^+$RORγt$^-$ cells (Figure 3B; Supplementary Figure S3D; Supplementary Table SXI). In contrast, SI NKp46$^+$RORγt$^+$ expressed as many fetal LTi genes as SI NKp46$^-$RORγt$^+$ cells (Supplementary Figure S3F), thus explaining why no preferential expression of the LTi gene set was observed when comparing these two subsets (Figure 3B). Finally, when comparing SI NKp46$^+$RORγt$^-$ with SI NKp46$^+$RORγt$^+$ ILCs, we observed a significant enrichment of the NK gene set in the former cell type (Figure 3A; Supplementary Figure S3G; Supplementary Table SX) and of the fetal LTi gene set in the latter (Figure 3B; Supplementary Figure S3H; Supplementary Table SXI). This confirmed that SI NKp46$^+$RORγt$^-$ cells were genetically closer to cNK cells than to their NKp46$^+$RORγt$^+$ SI counterpart. They will be therefore named SI NK cells thereafter. Reciprocally, SI NKp46$^+$RORγt$^+$ ILCs, when compared with SI NK cells, were preferentially enriched in *bona fide* fetal LTi genes.

We then analysed NK and fetal LTi genes enriched in SI NKp46$^+$ ILCs. For NK gene set, 19 out of 89 genes were shared by spleen and all SI NKp46$^+$ ILCs and encoded NK cell receptors (NKRs) (e.g. NKp46, NKR-P1C, NKG2C, NKG2E, NKG2D) or molecules involved in major NK cell functions (e.g. IFN-γ, Granzyme B) (Figure 3C; Supplementary Table SX). Genes shared only by spleen and SI NK cells ($n=13$) included *GzmA*, *Prf1*, *Eomes* and various *Klra*, all known to be involved in cNK cell functions. In contrast, known NK cell functions could be attributed only to very few genes common to splenic NK and SI NKp46$^+$RORγt$^+$ cells ($n=7$, e.g. *Fasl*) (Figure 3C; Supplementary Table SX). Remarkably, despite higher expression in both SI and spleen NKp46$^+$ ILCs as compared with SI NKp46$^-$RORγt$^+$ cells, several NK cell markers showed significant differences in their expression levels between NKp46$^+$ ILCs (Supplementary Figures S2F and S3I). This analysis confirmed the genetic proximity between spleen and SI NK cells and reveals an NKp46$^+$RORγt$^+$-specific NK cell signature. With respect to the fetal LTi gene set, SI NKp46$^+$ and NKp46$^-$ RORγt$^+$ ILCs shared the highest proportion of genes ($n=59$), including *Il1r1*, *Il22* and *Rorc* (Figure 3D; Supplementary Table SXI), thus revealing a molecular programme common to fetal LTi cells and adult RORγt$^+$ ILCs. In contrast, the function in SI ILCs remained largely to be unravelled for most of the genes from the LTi signature expressed to higher levels selectively in NKp46$^-$RORγt$^+$ ($n=42$) or in NKp46$^+$RORγt$^+$ ($n=21$) ILCs.

Impact of the commensal flora on SI NKp46$^+$ ILCs

In order to gain more insights into the biology of SI NKp46$^+$ ILCs, we investigated the factors that may modulate their development and function. SI NK cells were present at birth, while NKp46$^+$RORγt$^+$ cells only appeared after the first week of life, along with commensal flora exposure (Figure 4A). NKp46$^-$RORγt$^+$ cells were abundant in the intestine at day 16 of embryogenesis (E16.5) and still clearly detectable after birth. They were CD45^{int} and expressed high amounts of cell surface CD127 (IL-7Rα, data not shown), consistent with their LTi cell identity (Sawa *et al*, 2010). RORγt$^+$ ILCs were the major IL-22 producers in the gut in both fetal and early adult life (Figure 4B). NKp46$^+$ and NKp46$^-$ RORγt$^+$ ILCs were identified by using intracellular RORγt staining and expressed comparable amounts of RORγt protein (Figure 4A and B; Supplementary Figure S4A).

SI NKp46$^+$ ILCs developed normally in germ-free mice (Figure 4C). Furthermore, commensal flora depletion did not reduce, but rather increased, the ability of NKp46$^+$RORγt$^+$ cells to produce IL-22, in comparison to SI RORγt$^+$ ILCs isolated from conventional mice or recolonized germ mice

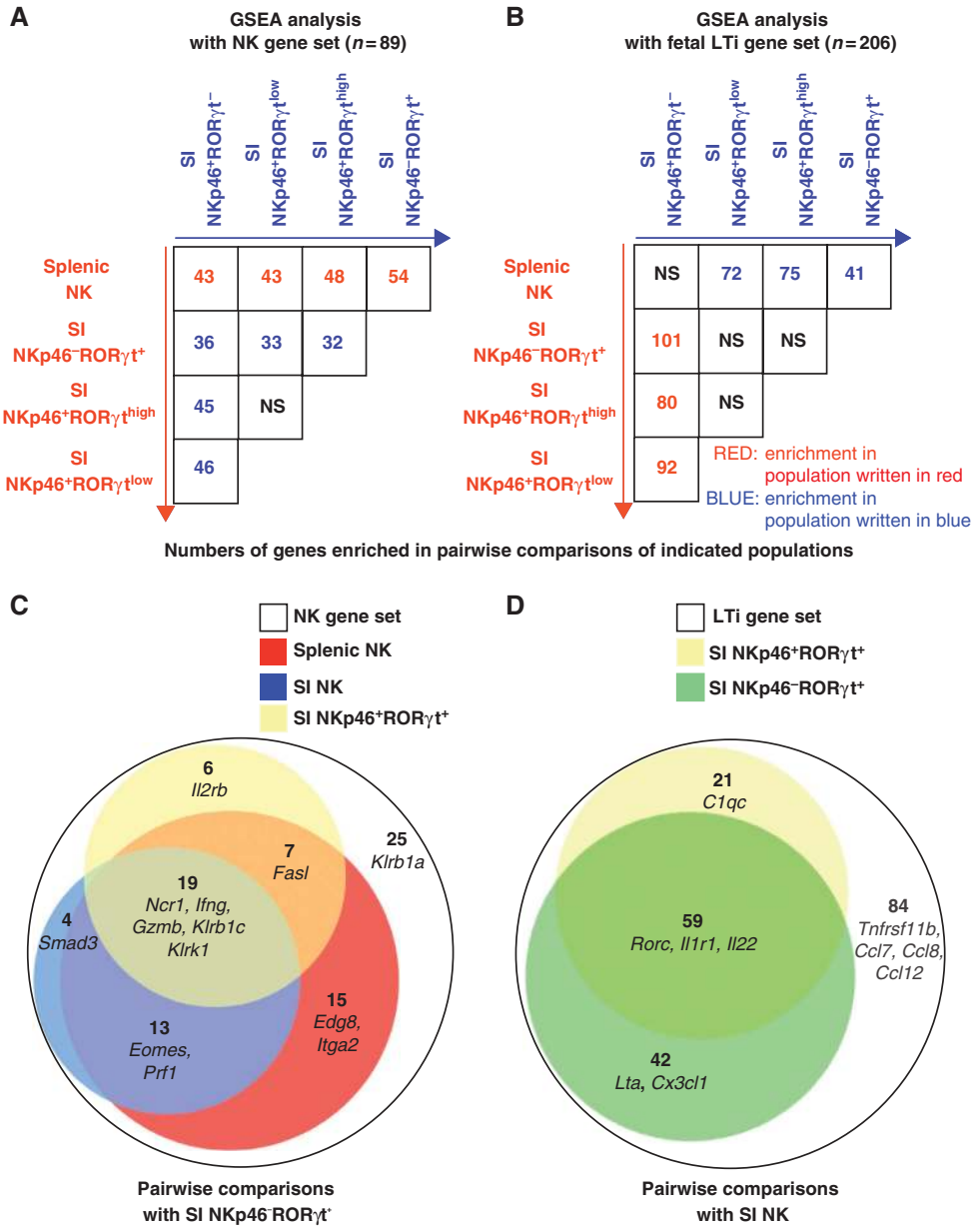

Figure 3 GSEA analysis of SI NKp46$^+$ cell subsets. (**A**, **B**) The numbers of genes differentially expressed in GSEA pairwise comparisons of indicated cell types, as explained in Supplementary data, using NK gene set ($n=89$, **A**) or fetal LTi gene set ($n=206$, **B**) are represented. Red colour corresponds to gene set enrichment in populations written in red, while blue colour corresponds to gene set enrichment in populations written in blue. NS, not significant. (**C**) Venn diagram of genes selected by GSEA analysis with NK gene set using results from pairwise comparisons of spleen NK (red), SI NK (blue) or SI NKp46$^+$RORγt$^+$ (yellow) with SI NKp46$^-$RORγt$^+$ cells (Supplementary Table SX). White area represents the genes that were not significantly enriched in the three pairwise comparisons indicated above. For each area, gene numbers and at least one representative gene are represented. (**D**) Venn diagram of genes selected by GSEA analysis with fetal LTi gene set using results from pairwise comparisons of SI NKp46$^+$RORγt$^+$ (yellow) or SI NKp46$^-$RORγt$^+$ (green) with SI NK cells (Supplementary Table SXI). White area represents the genes that were not significantly enriched in the two pairwise comparisons indicated above. For each area, gene numbers and at least one representative gene are represented.

(Figure 4D). Altogether, these results excluded a major requirement of commensal flora in driving the development and the acquisition of effectors functions of NKp46$^+$RORγt$^+$ cells, in contrast to earlier reports (Satoh-Takayama *et al*, 2008; Sanos *et al*, 2009).

Role of IL-1 on SI NKp46$^+$RORγt$^+$ and NKp46$^-$RORγt$^+$ cells

The MyD88 adaptor acts downstream of several receptors in the detection of both microbial and inflammatory stimuli, such as Toll-like receptors (TLRs) (Barton and Medzhitov, 2003) and the receptors for IL-1 and IL-18 (Sims, 2002; Schroder and Tschopp, 2010). We tested whether the development and/or the functions of SI NKp46$^+$ ILCs were dependent on MyD88 signalling. In MyD88$^{-/-}$ mice, we did not detect any significant alteration in the development of these cells (data not shown). However, both basal and IL-23-induced IL-22 productions by NKp46$^+$RORγt$^+$ and NKp46$^-$RORγt$^+$ ILCs were severely reduced in mutant mice, as compared with control littermates (Supplementary Figure S5A).

Within the intestine, both haematopoietic and non-haematopoietic cells, in particular epithelial cells, express MyD88-dependent receptors (Abreu, 2010). To determine in which cells MyD88 was required for IL-22 production by SI RORγt$^+$ ILCs, we analysed bone marrow chimera (BMC) mice for which donor and/or recipient mice were either wild type (WT) (CD45.1) or MyD88$^{-/-}$ (CD45.2). IL-22 production by NKp46$^+$RORγt$^+$ and NKp46$^-$RORγt$^+$ cells was more strongly reduced in MyD88$^{-/-}$→5.1 BMC mice than in reversed 5.1→MyD88$^{-/-}$ BMC mice (~80 versus ~20% of inhibition, respectively, as compared with 5.1→5.1 BMC mice) (Supplementary Figure S5B). Thus, MyD88 was required mainly in haematopoietic cells for the promotion of IL-22 production by both NKp46$^+$RORγt$^+$ and NKp46$^-$ RORγt$^+$ ILCs. Next, to determine whether the function of MyD88 for IL-22 production by RORγt$^+$ ILCs was cell autonomous, we analysed mixed BMC mice reconstituted with a mixture of CD45.1$^+$ WT and CD45.2$^+$ WT or MyD88$^{-/-}$

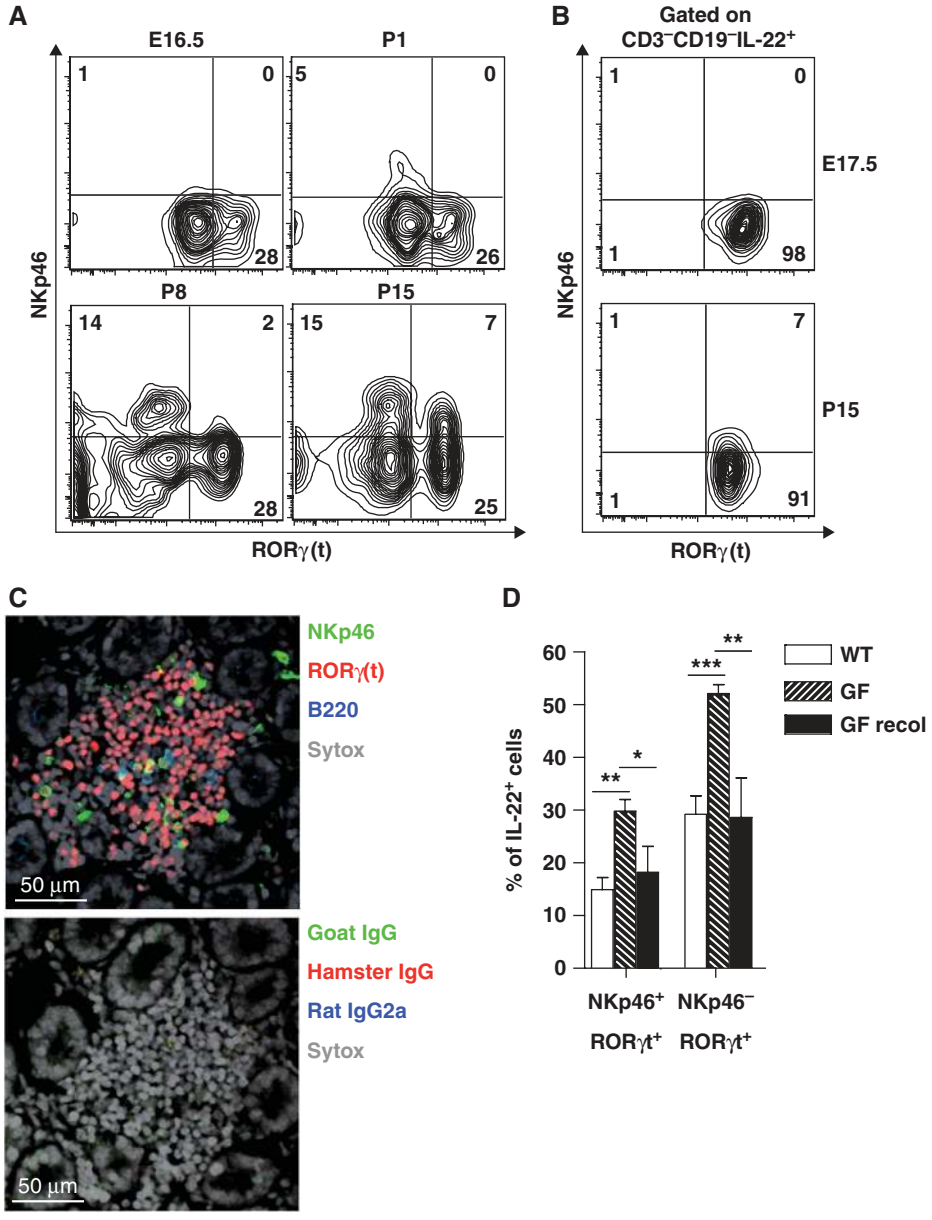

Figure 4 Impact of commensal flora on gut NKp46$^+$ ILC development and function. (**A**) Flow cytometry analysis of LPCs isolated from the whole intestine of C57BL/6 fetuses (E16.5 p.c.) or from SI of C57BL/6 newborns 1 day (P1), 1 week (P8) or 2 weeks (P15) after birth, by gating on CD45$^+$CD3$^-$CD19$^-$ cells. Numbers in quadrants indicate cell percentages. One experiment representative of two is depicted. (**B**) Flow cytometry analysis of LPCs isolated from the whole intestine of C57BL/6 fetuses (E17.5 p.c., top) or from SI of C57BL/6 newborns 2 weeks (P15, bottom) after birth, by gating on CD45$^+$CD3$^-$CD19$^-$ cells constitutively expressing IL-22. Numbers in quadrants indicate cell percentages. One experiment representative of two is shown. (**C**) Frozen sections of SI of C57BL/6 germ-free mice stained (top) with polyclonal anti-NKp46 serum (green), anti-RORγ supernatant hybridoma (red) and anti-B220 (blue) or (bottom) with indicated isotype control antibodies. Nuclei were counterstained with Sytox (grey). Scale bar = 50 µm. Data are representative of at least two independent experiments. (**D**) Percentages of IL-22$^+$ cells within indicated cell subsets were assessed by gating on CD45$^+$CD3$^-$CD19$^-$ cells. Before staining, SI LPCs were stimulated for 4 h in the presence of mouse IL-23 (40 ng/ml). White bars (WT) denote C57Bl/6 mice under conventional breeding conditions; striped bars (GF) denote C57Bl/6 germ-free mice; and black bars (GF recol) denote C57Bl/6 germ-free mice 5 weeks after recolonization by commensal flora. Data (mean ± s.e.m.) have been obtained using the following numbers of mice: WT = 5, GF = 5 and GF recol = 3. $^*P<0.05$, $^{**}P<0.005$, $^{***}P<0.0005$.

bone marrow precursors. IL-22 production was defective in MyD88$^{-/-}$ but not in WT RORγt$^+$ ILCs (Supplementary Figure S5C). Thus, MyD88 is required in both NKp46$^+$RORγt$^+$ and NKp46$^-$RORγt$^+$ ILCs for their ability to produce IL-22.

We then investigated the expression of MyD88-dependent receptors in NKp46$^+$RORγt$^+$ and NKp46$^-$RORγt$^+$ cells in our microarray data. While TLR expression was barely detectable, both cell subsets expressed high amounts of transcripts encoding IL-1R1, the receptor for IL-1α and IL-1β (Figure 5A; Supplementary Table SXI). IL-1β stimulation increased IL-22 production by NKp46$^+$RORγt$^+$ and NKp46$^-$RORγt$^+$ cells, both at steady state and upon IL-23 stimulation (Figure 5B). Moreover, both basal and cytokine-induced IL-22 productions were significantly reduced in the presence of anti-IL-1R1-blocking antibodies (Figure 5B). A severe defect in IL-22 production was detected in SI NKp46$^+$RORγt$^+$ and NKp46$^-$RORγt$^+$ cells isolated from IL-1R1$^{-/-}$ mice (Figure 5C). We then analysed mixed BMC mice reconstituted with a mixture of CD45.1$^+$ WT and CD45.2$^+$ WT or IL-1R1$^{-/-}$ bone marrow precursors. IL-22 production was significantly reduced in IL-1R1$^{-/-}$, but not in WT RORγt$^+$ ILCs isolated from these mixed BMC mice (Figure 5D), thus showing that the defect in IL-22 production in RORγt$^+$ ILCs of IL-1R1$^{-/-}$ mice was cell autonomous. Finally, anti-IL-1R1-blocking antibodies inhibited IL-22 production in gut RORγt$^+$ ILCs isolated from fetuses and from adult germ-free mice (Figure 5E).

Thus, the IL-1$\beta \rightarrow$IL-1R1$\rightarrow$MyD88 signalling pathway is critical for IL-22 production by mouse RORγt$^+$ ILCs, consistent with similar observations recently reported in humans (Cella *et al*, 2010; Hughes *et al*, 2010). This pathway is in place already starting in fetal life and does not require exposure to commensal flora.

Activation of SI NK and NKp46$^+$RORγt$^+$ cells by L.m.

We next investigated the function of SI NK, NKp46$^+$RORγt$^+$ and NKp46$^-$RORγt$^+$ ILCs in conditions of orally acquired bacterial infection. The natural route of *L. monocytogenes (L.m.)* infection in permissive hosts including humans, is oral (Hamon *et al*, 2006). *L.m.* is able to cross the intestinal barrier consecutive to the interaction between the bacterial invasin internalinA (InlA) and its receptor, E-cadherin, expressed on host epithelial cells (Lecuit *et al*, 2001). However, this mechanism is abrogated in mice due to a single amino-acid difference in E-cadherin, explaining why mice are resistant to oral *L.m.* infection. Sensitivity to oral *L.m.* infection can be conferred to mice upon ectopic expression of permissive human E-cadherin (Lecuit *et al*, 2001). Therefore, we took advantage of this transgenic (hEcad Tg) mouse model to investigate whether oral *L.m.* infection induced quantitative or qualitative modifications of SI NKp46$^+$ cell subsets. The percentages of SI NKp46$^+$ cell subsets were not substantially modified 24 h after oral *L.m.* infection (Figure 6A). However, as soon as 24 h after bacterial oral challenge, SI NK cells and NKp46$^+$RORγt$^+$ ILCs were induced to produce IFN-γ and IL-22, respectively (Figure 6B). Immunofluorescence stainings on tissue section showed that *L.m.* was found in both LP and PPs (Figure 6C). *L.m.* infection of PPs is mainly independent of InlA–E-cadherin interaction and results mostly from its translocation through M cells (Marco *et al*, 1997; Lecuit *et al*, 2007). Furthermore, InternalinA-deficient bacteria (Δ*inlA*) can induce intestinal immune responses similar to *wt L.m.* (Lecuit *et al*, 2007). These data prompted us to examine whether the activation of SI NKp46$^+$ cell subsets by oral *L.m.* infection could occur in the absence of InlA–E-cadherin interaction. Similar responses were observed in hEcad Tg mice upon oral infection with *wt* or with Δ*inlA L.m.* bacteria (Figure 6D), as well as in WT C57BL/6 mice infected with *wt L.m.* (Figure 7A and B). In C57BL/6 mice, SI NKp46$^+$RORγt$^+$ IL-22 and SI NK cell IFN-γ productions peaked at 48 h post-inoculation. Oral *L.m.* infection also enhanced IL-22 production by NKp46$^-$RORγt$^+$ cells, significantly above their constitutive level (Figure 7B). IFN-γ production was also induced in NK cells present in MLNs and, to lesser extent, in the spleen (Figure 7C). Forty-eight hours after oral *L.m.* inoculation, NKp46$^+$RORγt$^+$ and NKp46$^-$RORγt$^+$ ILCs were the main IL-22 producers within SI LP cells, while SI NK cells were an important source of IFN-γ (Supplementary Figure S6). Next, we examined whether these functions were required to control *L.m.* dissemination upon oral infection of WT C57BL/6 mice. Blocking IFN-γ, but not IL-22, with neutralizing antibodies induced significant increases in bacterial loads in the GALT (SI and MLNs) and in the spleen (Figure 7D and E). Therefore, IFN-γ, but not IL-22, critically contributed to the control of *L.m.* burden in the intestinal tissue and its dissemination to MLNs and spleen upon oral infection.

Discussion

Gut NKp46$^+$RORγt$^-$ and NKp46$^+$RORγt$^+$ cell subsets share the expression of some NKR, but exhibit different functional properties. Recent RORγt fate cell mapping studies proved their belonging to developmentally distinct lineages, as only RORγt$^+$ precursors, but not cNK cells, give rise to NKp46$^+$RORγt$^+$ cells (Satoh-Takayama *et al*, 2010; Sawa *et al*, 2010; Vonarbourg *et al*, 2010). However, the genetic programmes governing the distinct ontogeny and functions of gut NKp46$^+$ cell subsets have not been studied extensively. We described and analysed here the global gene expression programmes of both SI NKp46$^+$RORγt$^-$ and NKp46$^+$RORγt$^+$ cells. This large-scale unbiased approach confirmed at the transcriptional level the proximity between SI NKp46$^+$RORγt$^-$ cells and cNK cells on one side, and between SI NKp46$^+$RORγt$^+$ and NKp46$^-$RORγt$^+$ ILCs on the other side.

Combined expression of several NKRs and of various molecules required for NK cell-dependent cytotoxicity and cytokine/chemokine secretion, assigned SI NKp46$^+$RORγt$^-$ cells to the NK cell lineage. A quite different NKR repertoire was expressed by SI NKp46$^+$RORγt$^+$ cells, who were sharing a transcriptional signature with fetal LTi and adult NKp46$^-$RORγt$^+$ ILCs. In addition, NKp46$^+$RORγt$^+$ and NKp46$^-$RORγt$^+$ cells also shared a similar anatomical location. These data thus support a close proximity between these two cell types consistent with fate cell mapping studies (Satoh-Takayama *et al*, 2010; Sawa *et al*, 2010; Vonarbourg *et al*, 2010). Most of the molecules selectively expressed to high levels in NKp46$^+$RORγt$^+$ or NKp46$^-$RORγt$^+$ ILCs cannot currently be assigned to known RORγt$^+$ ILC-related functions. The identification of these lineage-specific 'signatures' will benefit the research community by opening novel avenues to unravel the whole extent of the functional specialization of these cells and their molecular regulation. These future studies should take in account also the recently

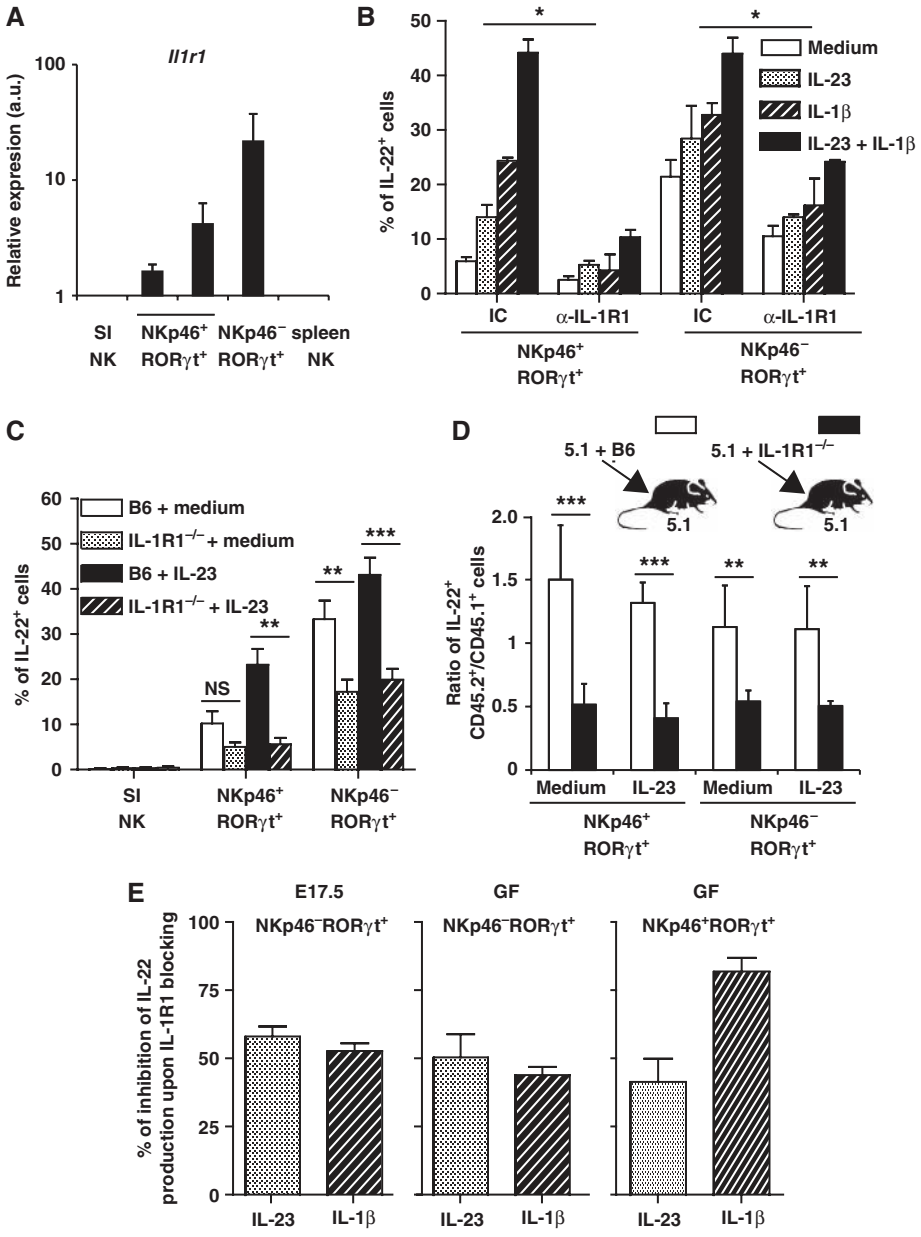

Figure 5 Role of IL-1R1/MyD88-dependent signalling in IL-22 production by NKp46$^+$RORγt$^+$ cells. (**A**) Relative expression of *Il1R1* transcript in indicated sorted cell subsets isolated from RORc(γt)$^{+/GFP}$ reporter mice was obtained upon quantitative real-time PCR. NKp46$^+$RORγt$^+$ cells included NKp46$^+$RORγt^{high} (right) and NKp46$^+$RORγt^{low} (left) cells. Data (mean ± s.e.m.) obtained from two independent experiments were normalized with respect to *Gapdh* (glyceraldehyde phosphate dehydrogenase) and expressed as arbitrary units. (**B**) IL-22$^+$ cell percentages (mean ± s.e.m.) within indicated SI LPC subsets of C57BL/6 mice after 4 h stimulation with medium = white bars; mouse IL-23 (40 ng/ml) = stippled bars; mouse IL-1β (40 ng/ml) = striped bars; mouse IL-23 and mouse IL-1β (both at 20 ng/ml) = black bars, in the presence of 20 μg/ml of isotype control hamster IgG (IC) or blocking anti-IL-1R1 (α-IL-1R1) antibodies. Data are representative of two independent experiments. (**C**) IL-22$^+$ cell percentages (mean ± s.e.m.) within indicated SI LPC subsets isolated from C57BL/6 (B6) mice or from IL-1R1$^{-/-}$ mice. Data are representative of two independent experiments. $N = 5$ for each group of mice. White bars = B6 + medium; stippled bars = IL-1R1$^{-/-}$ + medium; black bars = B6 + IL-23; striped bars = IL-1R1$^{-/-}$ + IL-23. NS, not significant. (**D**) IL-22$^+$ cell percentages (mean ± s.e.m.) within the indicated SI LPC subsets isolated from mixed BMC 5.1/B6 versus 5.1/IL-1R1$^{-/-}$ mice. Data are expressed as ratio of B6 versus 5.1 (white bars) or of IL-1R1$^{-/-}$ versus 5.1 (black bars) IL-22$^+$ cell percentages within each indicated subset. Data are representative of at least two independent experiments. (**E**) LPCs isolated from the whole gut of E17.5 C57Bl/6 fetuses or from SI of adult C57Bl/6 germ-free mice were stimulated with mouse IL-23 (40 ng/ml) = stippled bars or mouse IL-1β (40 ng/ml) = striped bars, in the presence of 20 μg/ml of isotype control hamster IgG (IC) or blocking anti-IL-1R1 (α-IL-1R1) antibodies. Data (mean ± s.e.m.) are expressed as percentage of inhibition of IL-22 production, obtained as following: {100 × [1−(% of IL-22$^+$ cells in the presence of α-IL-1R1 mAb/% of IL-22$^+$ cells in the presence of IC mAb)]}. Data are representative of two independent experiments. *$P<0.05$, **$P<0.005$, ***$P<0.0005$.

reported heterogeneity of adult NKp46$^-$RORγt$^+$ ILCs, including both CD4$^+$ and CD4$^-$ lin$^-$CD3$^-$CD127^{high}CD117^{high} LTi cells, as well as other lin$^-$CD3$^-$CD127^{dim}CD117^{dim} RORγt$^+$ ILCs (Sawa *et al*, 2010).

RORγt expression is stable in NKp46$^+$RORγt$^+$ cell residing in the SI, but it can be abrogated in cells located in the colon, the spleen and the LNs, leading to the generation of IFN-γ-polarized NKp46$^+$RORγt$^-$ cells phenotypically indistinguish-

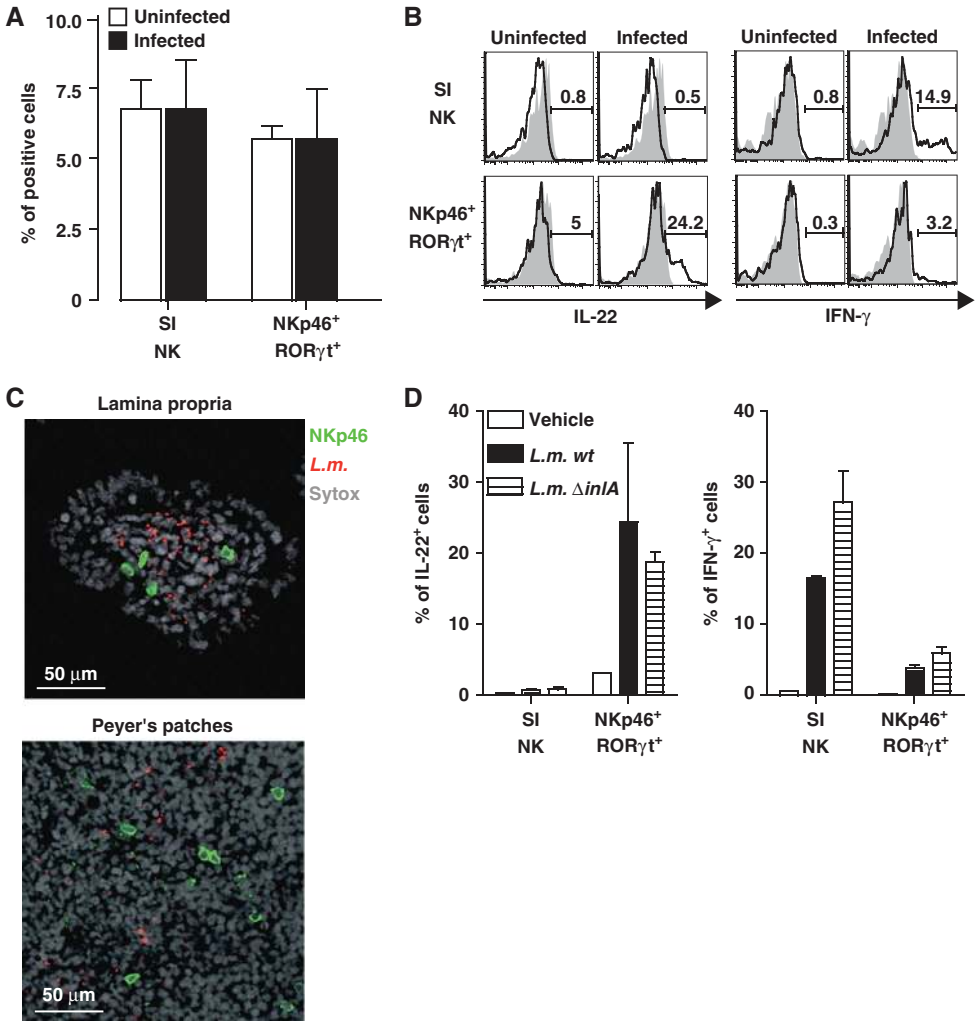

Figure 6 Activation of SI NKp46$^+$ILCs upon oral *L.m.* infection in hECad Tg mice. (**A**) Cell percentages (mean ± s.e.m.) of indicated SI NKp46$^+$ ILCs 24 h after oral gavage of hECad Tg mice with vehicle (uninfected, white bars) or with 10^{10} CFU of *L.m.* bacteria (infected, black bars) were analysed by flow cytometry, as depicted in Supplementary Figure S4B. Data are representative of at least two independent experiments. $N = 3$ for each mice group. (**B**) IL-22$^+$ and IFN-γ$^+$ cell percentages within indicated SI NKp46$^+$ ILCs obtained from vehicle-treated (uninfected) or infected hEcad tg mice were evaluated 24 h after oral *L.m.* gavage. Bold line denotes specific antibody and grey filled line denotes isotype-matched control antibody. One representative experiment of two is depicted. (**C**) Frozen tissue sections obtained from SI LP (top) and from PPs (bottom) of hEcad tg mice 24 h after oral *L.m.* infection were stained with polyclonal anti-NKp46 serum (green) and anti-*L.m.* serum (red). Nuclei were counterstained with Sytox (grey). Scale bar = 50 μm. Data are representative of at least two independent experiments. (**D**) IL-22$^+$ (left) or IFN-γ$^+$ (right) cell percentages (mean ± s.e.m.) in indicated SI NKp46$^+$ ILCs obtained from hEcad tg mice 24 h after oral *L.m.* infection. Vehicle-treated mice (vehicle, white bars); mice infected with WT *L.m.* (*L.m. wt*, black bars); mice infected with inlA-deficient *L.m.* bacteria (*L.m. ΔInlA*, striped bars). Data are representative of two independent experiments.

able from cNK cells (Vonarbourg *et al*, 2010). As our studies were performed with cells isolated exclusively from the SI, this rules out the risk of contamination of SI NK by NKp46$^+$RORγt$^-$ having downregulated RORγt expression. Comparison of the transcriptional profiles of the SI NKp46$^+$ cell subsets reported here with that of this new NKp46$^+$ RORγt$^-$ cell subset detectable in the colon and in lymphoid organs will be critical to identify the molecular mechanisms governing this unexpected tissue-specific RORγt-dependent functional switch.

The selective abundance of NKp46$^+$RORγt$^+$ cells in the SI suggested that gut-specific stimuli may drive and sustain their development. Consistently, previous studies reported that the development and the acquisition of effector functions of NKp46$^+$RORγt$^+$ cells were affected in germ-free mice (Satoh-Takayama *et al*, 2008; Sanos *et al*, 2009). We excluded a major role of gut microbiota in this function, as we showed that depletion of commensal bacteria did not affect NKp46$^+$RORγt$^+$ cell generation, consistent with a recent report (Sawa *et al*, 2010), even though it could reduce RORγt expression (Vonarbourg *et al*, 2010). IL-7 is currently the best-characterized stimulus regulating the development of NKp46$^+$RORγt$^+$ cells, which are severely reduced in both IL-7R-deficient mice and humans (Satoh-Takayama *et al*, 2010; Vonarbourg *et al*, 2010). In germ-free mice, IL-22 production by RORγt$^+$ ILCs was not affected, but rather increased. Consistently with our results, commensal flora-derived signals were recently reported to negatively regulate IL-22 production in RORγt$^+$ ILCs, through the induction of IL-25 secretion by gut epithelial cells (Sawa *et al*, 2011). Here, *in vivo* in mice, we demonstrated that IL-1R1 signalling is required for enabling IL-22 secretion in all gut RORγt$^+$ ILCs.

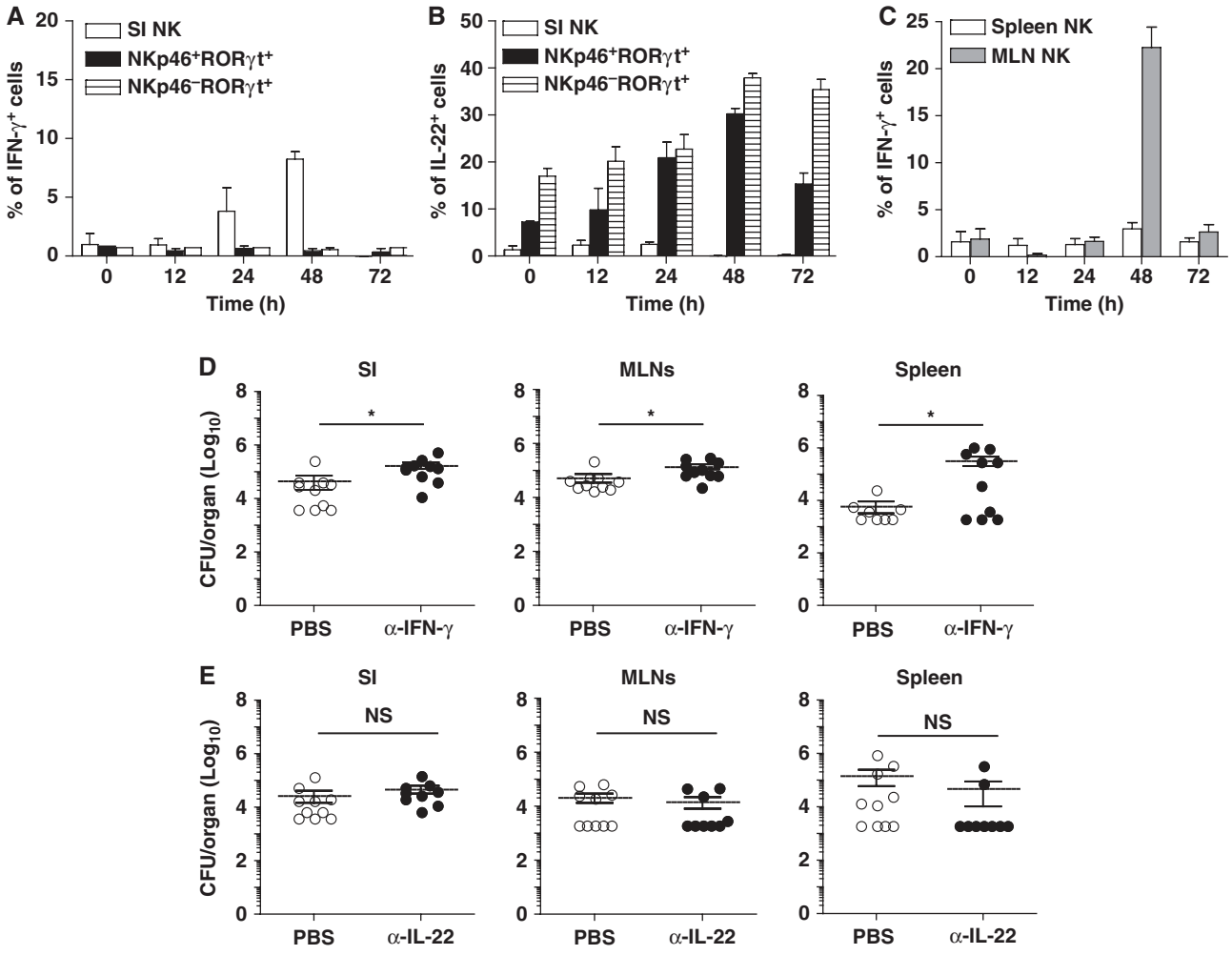

Figure 7 Activation of SI NKp46$^+$ ILCs upon oral *L.m.* infection in C57BL/6 mice. (**A**–**C**) IFN-γ^+ (**A**, **C**) or IL-22$^+$ (**B**) cell percentages (mean ± s.e.m.) in indicated SI, MLN or spleen cell subsets were analysed at indicated time points after oral *L.m.* infection in C57BL/6 mice. One representative experiment of three is shown. $N = 4$ for each time point. (**D**, **E**) CFU counts in the indicated organs were evaluated in anti-IFN-γ or anti-IL-22-treated C57BL/6 mice 48 h after oral *L.m.* infection. Data are representative of at least two independent experiments. (**D**) $N = 8$–10 for PBS-treated mice and $N = 10$ for anti-IFN-γ-treated mice. (**E**) $N = 10$ for PBS-treated mice and $N = 9$ for anti-IL-22-treated mice. $^*P < 0.05$. NS, not significant.

Responsiveness to IL-7 and IL-1β are thus critical for the physiological expansion of NKp46$^+$RORγt$^+$ cells and their acquisition of effector functions, consistent with recent human *in vitro* studies (Cella *et al*, 2010; Hughes *et al*, 2010). GSEA analyses highlighted IL-1R1 as a member of the fetal LTi signature conserved in all adult gut RORγt$^+$ ILCs, irrespective of NKp46 expression. Blocking IL-1R1 significantly reduced IL-22 production in both fetal and adult gut RORγt$^+$ ILCs, thus validating at the functional level our microarray data analysis. As IL-1R1-dependent signals also regulate Th17 cell expansion and function (Chung *et al*, 2009; Duan *et al*, 2010; Lee *et al*, 2010), IL-1β appears to be a master regulator for both innate and adaptive RORγt$^+$ effectors.

The molecular mechanisms through which IL-1R1 regulates IL-22 production are poorly characterized. In Th17 cells, IL-1R1 blockade or deficiency significantly reduces the expression of RORγt, IL-23R, IL-17 and IL-22 (Chung *et al*, 2009). However, RORγt protein was normally expressed in MyD88$^{-/-}$ and IL-1R1$^{-/-}$ ILCs (data not shown). The Aryl hydrocarbon receptor (AHR) could be another target of the signalling pathway downstream of IL-1R1. Indeed, AHR is required for IL-22 production in Th17 cells (Veldhoen *et al*, 2008) and, in the human counterparts of mouse NKp46$^+$RORγt$^+$ cells, IL-1β sustains *Ahr* and *Il22* expression (Hughes *et al*, 2010). Blocking IL-1R1 *in vitro* and *in vivo* severely compromised IL-22 production in RORγt$^+$ ILCs, including those isolated from fetuses and from germ-free mice. Thus, it is likely that signals independent of microbiota, but rather of host endogenous origin such as metabolic stress, could sustain basal levels of IL-1β. The gut stimuli responsible for the IL-1β-dependent IL-22 secretion remain to be characterized. Several microbial molecules as well as various host-derived compounds released upon cell damage can activate the inflammasome complex, thus inducing conversion of pro-IL-1β into secreted active IL-1β isoform (Sims, 2002; Dinarello, 2009; Schroder and Tschopp, 2010). Thus, upon gut injury, besides its well known direct pro-inflammatory function, increased IL-1β production might also exert a local healing and/or pro-inflammatory function via IL-22.

We showed that oral *L.m.* infection activated both SI NK and NKp46$^+$RORγt$^+$ cells according to their respective

polarization for the production of distinct cytokines as initially established in response to other stimuli. This observation validated *in vivo* the functional specialization of SI NKp46$^+$ ILC subsets as predicted from their gene expression profiles. Blocking IFN-γ, but not IL-22, significantly increased *L.m.* spreading from gut to systemic organs. We also showed that, when *L.m.* is administered in mice orally via its natural route of infection, SI NK cell-derived IFN-γ contributed to limit bacterial dissemination from gut to deeper tissues. In contrast to what was reported in *C. rodentium* infection (Satoh-Takayama *et al*, 2008; Zheng *et al*, 2008; Cella *et al*, 2009), IL-22 appeared dispensable for the control of oral *L.m.* infection. Hence, IL-22 can have different roles depending on the pathogens analysed, consistent with redundant or pathogenic functions of this cytokine in other microbial infections (Guo and Topham, 2010; Wilson *et al*, 2010). The contrasting roles of IL-22 for protection against epithelial infections may in part result from differences in the induction of local tissue injury depending on the pathogens examined. Specifically, *L.m.* breaches the intestinal epithelial barrier without significantly affecting its integrity (Lecuit *et al*, 2001), while *C. rodentium* infection causes extensive damage to the colonic epithelium, which requires the repair functions induced by IL-22 to prevent life-threatening pathology.

The critical contribution of NK cell-dependent IFN-γ secretion in controlling intravenous *L.m.* infection (Kang *et al*, 2008) and central nervous system listeriosis (Hayashi *et al*, 2009) in mice highlights a central role of NK cells in immunosurveillance against *L.m.* infection. It still remains to be determined whether, as reported in the case of intravenous infection (Pamer, 2004; Kang *et al*, 2008), NK cell-dependent IFN-γ secretion induced by *L.m.* infection via oral or cerebral route (Hayashi *et al*, 2009) is also crucial for the activation of inflammatory monocytes directly involved in *L.m.* elimination. In humans, *L.m.* infection is mostly limited to a benign gastroenteritis in immunocompetent individuals. However, *L.m.* can breach the blood–brain barrier and cause meningitis and encephalitis in immunocompromised patients, and the placental barrier in pregnant women, leading to fetal and neonatal infection (Lecuit, 2007). Our work thus contributes to further investigations on the role of tissue NK cells in the control of *L.m.* infection.

Materials and methods

Mice

C57BL/6 and congenic C57BL/6 Ly5.1 mice (CD45.1) were purchased from Charles River Laboratories, L'Arbesle, France, while C57BL/6 germ-free mice were obtained from Cryopréservation, Distribution, Typage et Archivage animal (CDTA), Orleans, France or were kindly provided by S Rabot, from Institut National de la Recherche Agronomique INRA, Jouy-en-Josas, France. Fetuses were obtained from pregnant C57BL/6 mice (16.5 or 17.5 days p. c.). All mutant mice used in this study were on C57BL/6 background. Rorc(γt)GFP mice were purchased from the Jackson Laboratory, USA. MyD88$^{-/-}$ mice were a gift of S Akira, Osaka, Japan, while IL-1R1$^{-/-}$ animals were kindly provided B Ryffel, Orleans, France. iFABP-hEcad transgenic (hEcad Tg) mice were generated by M Lecuit (Institut Pasteur, Paris, France). All mice were housed under specific pathogen-free conditions at the Laboratory Animal Facilities of the Centre d'Immunologie Marseille-Luminy or of the Institut Pasteur, Paris, France. Unless differently indicated, mice were used at 8–12 weeks of age. When control littermates were not available, mutant mice were cohoused at least 2 weeks with control C57BL/6 mice before performing the experiments. BMC mice were lethally irradiated (1000 rads), reconstituted with indicated bone marrow cells and analysed at least 8 weeks upon reconstitution. All experiments have been performed in accordance with the protocols approved by national regulation and the European Directives.

Flow cytometry

Cells were isolated from indicated organs as described in Supplementary data. Unless differently indicated, gut LP cells (LPCs) were isolated from SI. Before staining, cells were incubated for 10 min at 4°C with rat total immunoglobulins (5 μg/ml; Jackson Immuno Research, France). All the antibodies used were from BD Biosciences, with the exception of Pacific Blue-conjugated anti-mouse CD3 complex (17A2; Biolegend, France), PE-Cy7-conjugated anti-mouse CD45.1 (A20; Beckman Coulter) and PE-coupled anti-mouse NKp46 mAb (29A1.4; eBiosciences, France). For intracellular detection of IL-22 and IFN-γ cytokines, cells were plated in 24-well plates and stimulated in the presence of BrefeldinA 1 × (eBioscience) for 4 h at 37°C with indicated stimuli. At the end of stimulation, cells were fixed and permeabilized with the Foxp3 Fixation/Permeabilization kit (eBioscience), according to the manufacturer's indications. The same protocol was used for intracellular RORγt detection with an anti-mouse/human RORγt-PE (clone AFKJS-9; eBioscience). Intracellular IFN-γ staining was performed using PE-Cy7 or APC-conjugated anti-IFN-γ (XMG1.2; BD Pharmingen, France), while IL-22 was detected by using Alexa647-conjugated anti-mouse IL-22 (AM22.3, kindly provided by JC Renauld, Brussel, Belgium) in 1 × Permeabilization buffer (eBiosciences). Samples were run either on FACS Canto II or on LSRII cytometers (BD Biosciences, France) and analysed by using Flow Jo 9.0.2 software (Tree Star Inc.).

L.m. infection and bacterial count

L.m. WT reference strain EGD (*L.m.*, BUG 600) and isogenic *inlA* mutants (Δ*inlA*, BUG 947) were cultured to mid-log phase in brain–heart infusion (BHI) medium (BD Biosciences, France), then rinsed, re-suspended in PBS and frozen at −80°C. Inoculum concentration was determined upon 10-fold serial dilutions of thawed bacteria stock streaked on BHI-agar plates. After 12 h of starvation, C57BL/6 or hEcad Tg mice were inoculated by gavage with 10^{10} colony-forming units (CFU) of bacteria diluted in 0.5 ml of PBS containing 30 mg/ml of $CaCO_3$. Animals were killed at indicated times after infection. For detection of intracellular IFN-γ and IL-22 production, cells were extracted from indicated organs of uninfected and infected mice and incubated 4 h at 37°C with BrefeldinA 1 × (eBiosciences), without any other stimuli.

For *in vivo* cytokine-blocking experiments, C57BL/6 mice were injected intraperitoneally either with PBS (control) or with indicated cytokine-blocking antibodies (500 μg/mouse of purified anti-IFN-γ (XMG1.2), 750 μg/mouse of purified anti-IL-22 (AM22.3) at days −5, −2 and 0 of infection. For determination of bacterial CFU, 10-fold serial dilutions of homogenized SI, spleen and MLNs were streaked onto BHI-agar plates, followed by 2-day incubation at 37°C under aerobic conditions. Before homogenization, intestines were rinsed twice with DMEM and incubated for 2 h at room temperature in DMEM medium supplemented with gentamicin (100 μg/ml; Sigma, France).

Statistical analysis

Unpaired Student's *t*-test was used to compare the corresponding populations. $*P<0.05$, $**P<0.005$, $***P<0.0005$.

Detailed protocols regarding cell preparation, immunofluorescence staining, microarray data analysis and RT–qPCR are included in Supplementary data.

Supplementary data

Supplementary data are available at *The EMBO Journal* Online (http://www.embojournal.org).

Acknowledgements

We thank Lionel Chasson from the mouse functional genomics platform of Marseille-Nice Genopole for immunohistology; M Barad, P Grenot and A Zouine from CIML flow cytometry facility; M Fallet from CIML microscopy facility; all staff of CIML mouse house facilities. This work was supported by a grant funded by Agence Nationale de la Recherche (ANR-MIE 2008 N°R08063AS for ET, NY, EV, ML, OD and PC) and by institutional grants from INSERM, CNRS and Université de la Méditerranée to CIML. AR

was recipient of a doctoral fellowship cofunded by Region Provence Alpes Cote d'Azur and Institut National pour la Santé et la Recherche Medicale. EV is a scholar of the Institut Universitaire de France. All authors concur with the submission of the manuscript and none of the data have been previously reported or are under consideration for publication elsewhere.

Author contributions: ET and EV designed the experiments and wrote the paper; AR, NY and ET designed, performed and analysed the experiments; AF bred and took care of the majority of mice used in the experiments; CA and GN contributed to first infection experiments; TPVM, MD and BE contributed to microarray analysis; JCR, OD, PC and ML provided reagents crucial for the experiments and contributed to the design of the experiments and the interpretation of the data.

Conflict of interest

EV is a cofounder and shareholder of Innate-Pharma. The other authors declare that they have no conflict of interest.

References

Abreu MT (2010) Toll-like receptor signalling in the intestinal epithelium: how bacterial recognition shapes intestinal function. *Nat Rev Immunol* **10:** 131–144

Barton GM, Medzhitov R (2003) Toll-like receptor signaling pathways. *Science* **300:** 1524–1525

Buonocore S, Ahern PP, Uhlig HH, Ivanov II, Littman DR, Maloy KJ, Powrie F (2010) Innate lymphoid cells drive interleukin-23-dependent innate intestinal pathology. *Nature* **464:** 1371–1375

Cella M, Fuchs A, Vermi W, Facchetti F, Otero K, Lennerz JK, Doherty JM, Mills JC, Colonna M (2009) A human natural killer cell subset provides an innate source of IL-22 for mucosal immunity. *Nature* **457:** 722–725

Cella M, Otero K, Colonna M (2010) Expansion of human NK-22 cells with IL-7, IL-2, and IL-1beta reveals intrinsic functional plasticity. *Proc Natl Acad Sci USA* **107:** 10961–10966

Chung Y, Chang SH, Martinez GJ, Yang XO, Nurieva R, Kang HS, Ma L, Watowich SS, Jetten AM, Tian Q, Dong C (2009) Critical regulation of early Th17 cell differentiation by interleukin-1 signaling. *Immunity* **30:** 576–587

Crellin NK, Trifari S, Kaplan CD, Cupedo T, Spits H (2010) Human NKp44 + IL-22 + cells and LTi-like cells constitute a stable RORC + lineage distinct from conventional natural killer cells. *J Exp Med* **207:** 281–290

Cupedo T, Crellin NK, Papazian N, Rombouts EJ, Weijer K, Grogan JL, Fibbe WE, Cornelissen JJ, Spits H (2009) Human fetal lymphoid tissue-inducer cells are interleukin 17-producing precursors to RORC(+) CD127(+) natural killer-like cells. *Nat Immunol* **10:** 66–74

Dinarello CA (2009) Immunological and inflammatory functions of the interleukin-1 family. *Annu Rev Immunol* **27:** 519–550

Duan J, Chung H, Troy E, Kasper DL (2010) Microbial colonization drives expansion of IL-1 receptor 1-expressing and IL-17-producing gamma/delta T cells. *Cell Host Microbe* **7:** 140–150

Eberl G, Marmon S, Sunshine MJ, Rennert PD, Choi Y, Littman DR (2004) An essential function for the nuclear receptor RORgamma(t) in the generation of fetal lymphoid tissue inducer cells. *Nat Immunol* **5:** 64–73

Guo H, Topham DJ (2010) Interleukin-22 (IL-22) production by pulmonary natural killer cells and the potential role of IL-22 during primary influenza virus infection. *J Virol* **84:** 7750–7759

Hamon M, Bierne H, Cossart P (2006) Listeria monocytogenes: a multifaceted model. *Nat Rev Microbiol* **4:** 423–434

Hayashi T, Nagai S, Fujii H, Baba Y, Ikeda E, Kawase T, Koyasu S (2009) Critical roles of NK and CD8 + T cells in central nervous system listeriosis. *J Immunol* **182:** 6360–6368

Hughes T, Becknell B, Freud AG, McClory S, Briercheck E, Yu J, Mao C, Giovenzana C, Nuovo G, Wei L, Zhang X, Gavrilin MA, Wewers MD, Caligiuri MA (2010) Interleukin-1beta selectively expands and sustains interleukin-22 + immature human natural killer cells in secondary lymphoid tissue. *Immunity* **32:** 803–814

Hughes T, Becknell B, McClory S, Briercheck E, Freud AG, Zhang X, Mao H, Nuovo G, Yu J, Caligiuri MA (2009) Stage 3 immature human natural killer cells found in secondary lymphoid tissue constitutively and selectively express the TH 17 cytokine interleukin-22. *Blood* **113:** 4008–4010

Ivanov II, Diehl GE, Littman DR (2006) Lymphoid tissue inducer cells in intestinal immunity. *Curr Top Microbiol Immunol* **308:** 59–82

Ivanov II, Frutos Rde L, Manel N, Yoshinaga K, Rifkin DB, Sartor RB, Finlay BB, Littman DR (2008) Specific microbiota direct the differentiation of IL-17-producing T-helper cells in the mucosa of the small intestine. *Cell Host Microbe* **4:** 337–349

Iwasaki A (2007) Mucosal dendritic cells. *Annu Rev Immunol* **25:** 381–418

Kang SJ, Liang HE, Reizis B, Locksley RM (2008) Regulation of hierarchical clustering and activation of innate immune cells by dendritic cells. *Immunity* **29:** 819–833

Lecuit M (2007) Human listeriosis and animal models. *Microbes Infect* **9:** 1216–1225

Lecuit M, Sonnenburg JL, Cossart P, Gordon JI (2007) Functional genomic studies of the intestinal response to a foodborne enteropathogen in a humanized gnotobiotic mouse model. *J Biol Chem* **282:** 15065–15072

Lecuit M, Vandormael-Pournin S, Lefort J, Huerre M, Gounon P, Dupuy C, Babinet C, Cossart P (2001) A transgenic model for listeriosis: role of internalin in crossing the intestinal barrier. *Science* **292:** 1722–1725

Lee WW, Kang SW, Choi J, Lee SH, Shah K, Eynon EE, Flavell RA, Kang I (2010) Regulating human Th17 cells via differential expression of IL-1 receptor. *Blood* **115:** 530–540

Luci C, Reynders A, Ivanov II, Cognet C, Chiche L, Chasson L, Hardwigsen J, Anguiano E, Banchereau J, Chaussabel D, Dalod M, Littman DR, Vivier E, Tomasello E (2009) Influence of the transcription factor RORgammat on the development of NKp46(+) cell populations in gut and skin. *Nat Immunol* **10:** 75–82

Marco AJ, Altimira J, Prats N, Lopez S, Dominguez L, Domingo M, Briones V (1997) Penetration of Listeria monocytogenes in mice infected by the oral route. *Microb Pathog* **23:** 255–263

Mebius RE (2003) Organogenesis of lymphoid tissues. *Nat Rev Immunol* **3:** 292–303

Moro K, Yamada T, Tanabe M, Takeuchi T, Ikawa T, Kawamoto H, Furusawa J, Ohtani M, Fujii H, Koyasu S (2010) Innate production of T(H)2 cytokines by adipose tissue-associated c-Kit(+)Sca-1(+) lymphoid cells. *Nature* **463:** 540–544

Neill DR, Wong SH, Bellosi A, Flynn RJ, Daly M, Langford TK, Bucks C, Kane CM, Fallon PG, Pannell R, Jolin HE, McKenzie AN (2010) Nuocytes represent a new innate effector leukocyte that mediates type-2 immunity. *Nature* **464:** 1367–1370

Pamer EG (2004) Immune responses to Listeria monocytogenes. *Nat Rev Immunol* **4:** 812–823

Saenz SA, Siracusa MC, Perrigoue JG, Spencer SP, Urban Jr JF, Tocker JE, Budelsky AL, Kleinschek MA, Kastelein RA, Kambayashi T, Bhandoola A, Artis D (2010) IL25 elicits a multipotent progenitor cell population that promotes T(H)2 cytokine responses. *Nature* **464:** 1362–1366

Sanos SL, Bui VL, Mortha A, Oberle K, Heners C, Johner C, Diefenbach A (2009) RORgammat and commensal microflora are required for the differentiation of mucosal interleukin 22-producing NKp46(+) cells. *Nat Immunol* **10:** 83–91

Satoh-Takayama N, Lesjean-Pottier S, Vieira P, Sawa S, Eberl G, Vosshenrich CA, Di Santo JP (2010) IL-7 and IL-15 independently program the differentiation of intestinal CD3-NKp46 + cell subsets from Id2-dependent precursors. *J Exp Med* **207:** 273–280

Satoh-Takayama N, Vosshenrich CA, Lesjean-Pottier S, Sawa S, Lochner M, Rattis F, Mention JJ, Thiam K, Cerf-Bensussan N, Mandelboim O, Eberl G, Di Santo JP (2008) Microbial flora drives interleukin 22 production in intestinal NKp46 + cells that provide innate mucosal immune defense. *Immunity* **29:** 958–970

Sawa S, Cherrier M, Lochner M, Satoh-Takayama N, Fehling HJ, Langa F, Di Santo JP, Eberl G (2010) Lineage relationship analysis of RORgammat + innate lymphoid cells. *Science* **330:** 665–669

Sawa S, Lochner M, Satoh-Takayama N, Dulauroy S, Berard M, Kleinschek M, Cua D, Di Santo JP, Eberl G (2011) RORgammat(+) innate lymphoid cells regulate intestinal homeostasis by integrating negative signals from the symbiotic microbiota. *Nat Immunol* **12:** 320–326

Schroder K, Tschopp J (2010) The inflammasomes. *Cell* **140:** 821–832

Sims JE (2002) IL-1 and IL-18 receptors, and their extended family. *Curr Opin Immunol* **14:** 117–122

Spits H, Di Santo JP (2011) The expanding family of innate lymphoid cells: regulators and effectors of immunity and tissue remodeling. *Nat Immunol* **12:** 21–27

Swamy M, Jamora C, Havran W, Hayday A (2010) Epithelial decision makers: in search of the 'epimmunome'. *Nat Immunol* **11:** 656–665

Takatori H, Kanno Y, Watford WT, Tato CM, Weiss G, Ivanov II, Littman DR, O'Shea JJ (2009) Lymphoid tissue inducer-like cells are an innate source of IL-17 and IL-22. *J Exp Med* **206:** 35–41

Takayama T, Kamada N, Chinen H, Okamoto S, Kitazume MT, Chang J, Matuzaki Y, Suzuki S, Sugita A, Koganei K, Hisamatsu T, Kanai T, Hibi T (2010) Imbalance of NKp44(+)NKp46(−) and NKp44(−)NKp46(+) natural killer cells in the intestinal mucosa of patients with Crohn's disease. *Gastroenterology* **139:** 882–892, e881–e883

Veldhoen M, Hirota K, Westendorf AM, Buer J, Dumoutier L, Renauld JC, Stockinger B (2008) The aryl hydrocarbon receptor links TH17-cell-mediated autoimmunity to environmental toxins. *Nature* **453:** 106–109

Vivier E, Spits H, Cupedo T (2009) Interleukin-22-producing innate immune cells: new players in mucosal immunity and tissue repair? *Nat Rev Immunol* **9:** 229–234

Vonarbourg C, Mortha A, Bui VL, Hernandez PP, Kiss EA, Hoyler T, Flach M, Bengsch B, Thimme R, Holscher C, Honig M, Pannicke U, Schwarz K, Ware CF, Finke D, Diefenbach A (2010) Regulated expression of nuclear receptor RORgammat confers distinct functional fates to NK cell receptor-expressing RORgammat(+) innate lymphocytes. *Immunity* **33:** 736–751

Wilson MS, Feng CG, Barber DL, Yarovinsky F, Cheever AW, Sher A, Grigg M, Collins M, Fouser L, Wynn TA (2010) Redundant and pathogenic roles for IL-22 in mycobacterial, protozoan, and helminth infections. *J Immunol* **184:** 4378–4390

Wolk K, Witte E, Witte K, Warszawska K, Sabat R (2010) Biology of interleukin-22. *Semin Immunopathol* **32:** 17–31

Zenewicz LA, Yancopoulos GD, Valenzuela DM, Murphy AJ, Stevens S, Flavell RA (2008) Innate and adaptive interleukin-22 protects mice from inflammatory bowel disease. *Immunity* **29:** 947–957

Zheng Y, Valdez PA, Danilenko DM, Hu Y, Sa SM, Gong Q, Abbas AR, Modrusan Z, Ghilardi N, de Sauvage FJ, Ouyang W (2008) Interleukin-22 mediates early host defense against attaching and effacing bacterial pathogens. *Nat Med* **14:** 282–289